

Licochalcone E has an antidiabetic effect

Hong Gyu Park^{a,b,1,2}, Eun Jung Bak^{c,1}, Gye-Hyeong Woo^d, Jin Moon Kim^{a,e}, Zhejiu Quan^c, Jung Mogg Kim^b,
Ho-Kun Yoon^f, Seung Hoon Cheon^g, Goo Yoon^h, Yun-Jung Yoo^{a,e}, Younghwa Na^{i,*}, Jeong-Heon Cha^{a,c,e,*}

^aDepartment of Oral Biology, BK21 Project, Oral Science Research Center, Yonsei University College of Dentistry, Seoul, Republic of Korea

^bDepartment of Microbiology and Institute of Biomedical Science, Hanyang University College of Medicine, Seoul, Republic of Korea

^cOral Cancer Research Institute, Yonsei University College of Dentistry, Seoul, Republic of Korea

^dDepartment of Clinical Laboratory Science, Semyung University, Jecheon, Republic of Korea

^eDepartment of Applied Life Science, The Graduate School, Yonsei University, Seoul, Republic of Korea

^fDepartment of Biochemistry and Molecular Biology, Center for Chronic Metabolic Disease Research, College of Medicine, Yonsei University, Seoul, Republic of Korea

^gCollege of Pharmacy and Research Institute of Drug Development, Chonnam National University, Gwangju, Republic of Korea

^hCollege of Pharmacy, Mokpo National University, Mu-an-gun, Republic of Korea

ⁱCollege of Pharmacy, CHA University, Seoul, Republic of Korea

Received 26 May 2010; received in revised form 3 March 2011; accepted 25 March 2011

Abstract

Licochalcone E (lico E) is a retrochalcone isolated from the root of *Glycyrrhiza inflata*. Retrochalcone compounds evidence a variety of pharmacological profiles, including anticancer, antiparasitic, antibacterial, antioxidative and superoxide-scavenging properties. In this study, we evaluated the biological effects of lico E on adipocyte differentiation *in vitro* and obesity-related diabetes *in vivo*. We employed 3T3-L1 preadipocyte and C3H10T1/2 stem cells for *in vitro* adipocyte differentiation study and diet-induced diabetic mice for *in vivo* study. The presence of lico E during adipogenesis induced adipocyte differentiation to a significant degree, particularly at the early induction stage. Licochalcone E evidenced weak, but significant, peroxisome proliferator-activated receptor gamma (PPAR γ) ligand-binding activity. Two weeks of lico E treatment lowered blood glucose levels and serum triglyceride levels in the diabetic mice. Additionally, treatment with lico E resulted in marked reductions in adipocyte size and increases in the mRNA expression levels of PPAR γ in white adipose tissue (WAT). Licochalcone E was also shown to significantly stimulate Akt signaling in epididymal WAT. In conclusion, lico E increases the levels of PPAR γ expression, at least in part, via the stimulation of Akt signals and functions as a PPAR γ partial agonist, and this increased PPAR γ expression enhances adipocyte differentiation and increases the population of small adipocytes, resulting in improvements in hyperglycemia and hyperlipidemia under diabetic conditions.

© 2012 Elsevier Inc. All rights reserved.

Keywords: Licochalcone E; Adipocyte differentiation; Obesity; Diabetes

1. Introduction

Type 2 diabetes is a metabolic disorder characterized as secondary hyperglycemia by insulin resistance and caused by multifactorial etiology, including environmental factors, particularly diet and genetic components. The relationship between obesity and type 2 diabetes has been known for decades, and the major basis for this link is the ability of obesity to induce insulin resistance. Adipose tissue is

an important organ for both glucose and lipid metabolism. Insulin resistance is associated with a deficiency of adipose tissue under conditions of lipodystrophy [1], as well as the accumulation of adipose tissue under obesity conditions [2–4]. Kim et al. previously reported that mice lacking adipose tissue were diabetic and severely insulin resistant and evidenced hugely elevated triglyceride contents in the liver and skeletal muscles. The results of these studies demonstrate that altered or impaired adipocyte differentiation may promote the development of insulin resistance, ultimately resulting in type 2 diabetes. Thus, studies of adipocyte differentiation in cell culture as well as animal models have been used as models for the testing of insulin sensitivity and novel antidiabetic drugs.

Two major *in vitro* model systems have been exploited in order to evaluate adipocyte differentiation. One model employs preadipocyte cell lines that can be induced to terminally differentiate into adipocytes, but not into other cell types. 3T3-L1 is the most extensively utilized and well-characterized preadipocyte cell line [5–7]. The other model involves the use of multipotent stem cell lines that have yet to undergo commitment to an adipocyte lineage, including the C3H10T1/

* Corresponding authors. Jeong-Heon Cha is to be contacted at Tel.: +82 2 2228 3061; fax: +82 2 2227 7903. Younghwa Na, Tel.: +82 2 555 4076; fax: +82 2 555 6689.

E-mail addresses: yna7315@cha.ac.kr (Y. Na), jcha@yuhs.ac (J.-H. Cha).

¹ Author contributions: Hong Gyu Park and Eun Jung Bak contributed equally to this work.

² Present address for Hong Gyu Park: ATGC Biotechnology Co., Ltd., Flat 604, Eulji Bldg, 212 Yangji-Dong, Sujeong-Gu, Seongnam-Si, Gyeonggi-Do, Republic of Korea.

2 murine cell line, which is the most frequently utilized cell line [8,9] for studies of the differentiation of stem cells into adipocytes [10].

Peroxisome proliferator-activated receptor (PPAR) γ performs a key role in glucose and lipid metabolism and is a critical transcription factor in adipocyte differentiation. It has been previously reported that small adipocytes take up more glucose than do large adipocytes, whereas large adipocytes induce impairments in intracellular glucose metabolism, thereby resulting in reductions of glucose oxidation in adipocytes [11]. The increased population of small adipocytes via the activation of PPAR γ by treatment with thiazolidinediones, which are PPAR γ agonists, may account for the observed improvements in insulin sensitivity and the reduction in fatty acid levels, thereby resulting in the amelioration of diabetic status [12,13].

Licorice, the root and stolon of the *Glycyrrhiza* plant species (Leguminosae) including *G. inflata* Batalin, *G. uralensis* Fischer and *G. glabra* Linne, has been used as medicinal and sweetening agents in food products. Each species harbors species-specific flavonoids. Retrochalcones are an unusual phenolic compound family. *G. inflata* is the major source of six retrochalcone compounds: licochalcone (lico) A–E and echinatin. They have demonstrated a variety of

pharmacological profiles including anticancer, antibacterial, antioxidative and anti-inflammatory effects [14–17]. Licochalcone E has been recently isolated, and its biological activities have yet to be elucidated [17,18]. Therefore, we evaluated the biological activities of lico E and, in this study, identified and characterized its novel effects on adipocyte differentiation *in vitro* and in a diabetic model *in vivo*.

2. Materials and methods

2.1. Cell culture and adipocyte differentiation

3T3-L1 cells (American Type Culture Collection, Rockville, MD, USA) were grown in Dulbecco's modified Eagle's medium (DMEM) including 10% bovine calf serum (BCS), 100 U/ml penicillin and 100 μ g/ml streptomycin in a humidified incubator under an atmosphere of 5% CO₂ and at a temperature of 37°C. C3H10T1/2 cells (American Type Culture Collection) were cultured in DMEM containing 10% fetal bovine serum (FBS). The cells were differentiated in accordance with a well-established standard adipocyte differentiation protocol [19,20]. In brief, 3T3-L1 cells at 2 days postconfluence (day 0) were stimulated to differentiate in a standard adipogenic medium (DMEM containing 10% FBS, 0.5 μ M isobutylmethylxanthine, 1 μ M dexamethasone and 1 μ g/ml of insulin) for 2 days. The differentiation medium was replaced after 2 days with DMEM containing 10% FBS and 1 μ g/ml of insulin, then exchanged every other day with DMEM containing 10% FBS. During adipocyte differentiation, 3T3-L1 cells were treated with

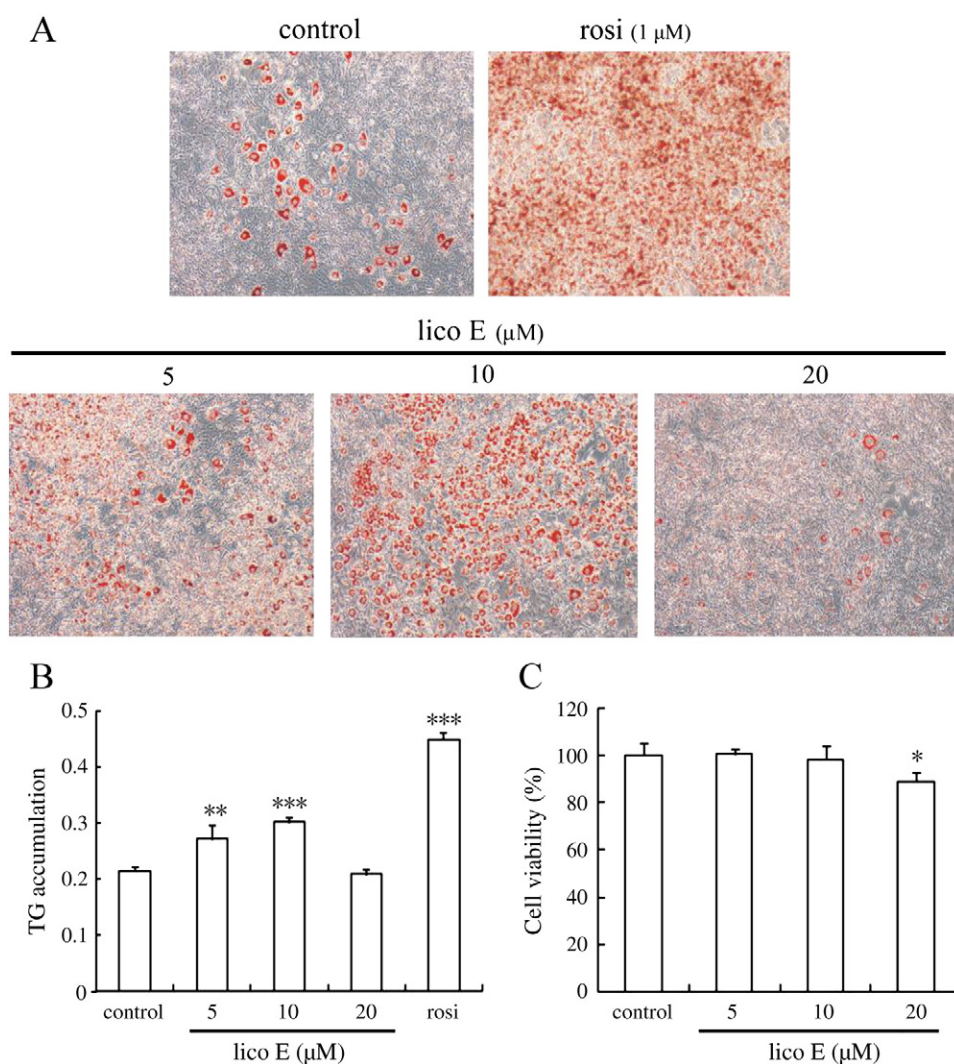


Fig. 1. Effects of lico E on adipocyte differentiation in 3T3-L1. (A) 3T3-L1 cells were treated with lico E (0, 5, 10 or 20 μ M) during adipocyte differentiation for 8 days. Control was differentiated by standard adipogenic induction media without other treatment. 3T3-L1 adipogenesis was visualized by Oil Red O staining. Microscopic pictures were taken at day 8 with $\times 100$ magnification. (B) The stained Oil Red O was extracted with isopropanol. The absorbance of the extracted Oil Red O was spectrophotometrically determined at 570 nm in order to measure triglyceride accumulation. (C) To investigate the toxicity of lico E on cell viability, 3T3-L1 was incubated in the presence of lico E at a concentration of 0, 5, 10 or 20 μ M, and the cell viability was evaluated via MTT assays after 48 h. The error bars represent the standard error of the mean. The symbols *, ** and *** indicate significant difference at $P < .05$, $P < .01$ and $P < .001$, respectively. TG, triglyceride.

lico E at a concentration of 0, 5, 10 or 20 μM from days 0 to 8, then treated with 1 μM rosiglitazone (rosi) as a positive control. C3H10T1/2 cells were stimulated to differentiate via the aforementioned method, except that 10% FBS was utilized rather than 10% BCS in the media prior to induction. During adipocyte differentiation, C3H10T1/2 cells were treated with lico E at a concentration of 0, 5, 10 or 25 μM for 8 days during a standard adipogenic induction. For the time-course study, C3H10T1/2 cells were induced in the presence of 10 μM lico E for various periods during adipocyte differentiation. In order to examine effects of Akt inhibitor, C3H10T1/2 cells were pretreated with 10 μM Akt inhibitor 124005 (Calbiochem, La Jolla, CA, USA) for 1 h before the cells were stimulated to differentiate in the standard adipocyte medium containing 10 μM lico E and 10 μM Akt inhibitor. All assays were conducted in triplicate, and at least three separate assays were performed.

2.2. Quantification of lipid accumulation

In order to determine the degree of differentiation and to visualize lipid accumulation, cytoplasmic triglycerides in the cells were stained with Oil Red O (Sigma-Aldrich, St. Louis, MO, US) as previously described [20,21]. The stained cells were photographed at a magnification of $\times 100$ using an Olympus CKX41 inverted microscope system (Tokyo, Japan). After the Oil Red O retained in the cells was extracted with isopropanol, the absorbance was determined spectrophotometrically at 570 nm using an MRX II microplate reader (Dynatech Labs., Chantilly, VA, USA).

2.3. 3-(4,5-Dimethylthiazol-2-yl)2,5-diphenyl tetrazolium bromide (MTT) assay

The cells (5×10^4 cells/well) were plated and incubated for 24 h in 96-well plates. The cells were subsequently treated for 48 h with various concentrations of lico E. 3-(4,5-Dimethylthiazol-2-yl)2,5-diphenyl tetrazolium bromide (Sigma-Aldrich, St. Louis, MO, USA) was employed to determine the cell viability in accordance with the manufacturer's instructions. The absorbance at 570 nm was measured with an MRX II microplate reader (Dynatech Labs, Chantilly, VA, USA).

2.4. Luciferase reporter gene assay

CV1 cells (monkey kidney cell line; ATCC CCL70) were cultured in DMEM including 10% FBS, 100 U/ml penicillin and 100 $\mu\text{g}/\text{ml}$ streptomycin in a humidified incubator at 5% CO_2 and 37°C. The luciferase reporter gene assay conducted to determine the degree of PPAR γ transactivation was conducted as previously described [22]. In brief, CV1 cells (1.5×10^5 cells/well) were plated on six-well plates, and 24 h later, the cells were co-transfected with 500 ng of pUSA-luciferase, 100 ng of GAL4PPAR γ LBD and 100 ng of CMV β -galactosidase using Lipofectamine PLUS reagent (Invitrogen, Carlsbad, CA, USA) in DMEM including 100 U/ml penicillin and 100 $\mu\text{g}/\text{ml}$ streptomycin. Transfected cells after 24 h were treated either with vehicle or with lico E at a concentration of 0, 5, 10 or 20 μM . Luciferase activity was measured after 24 h using a luciferase substrate kit (Promega, Madison, WI, USA) and a Microumat Plus LB96V luminometer (ALT, PA,

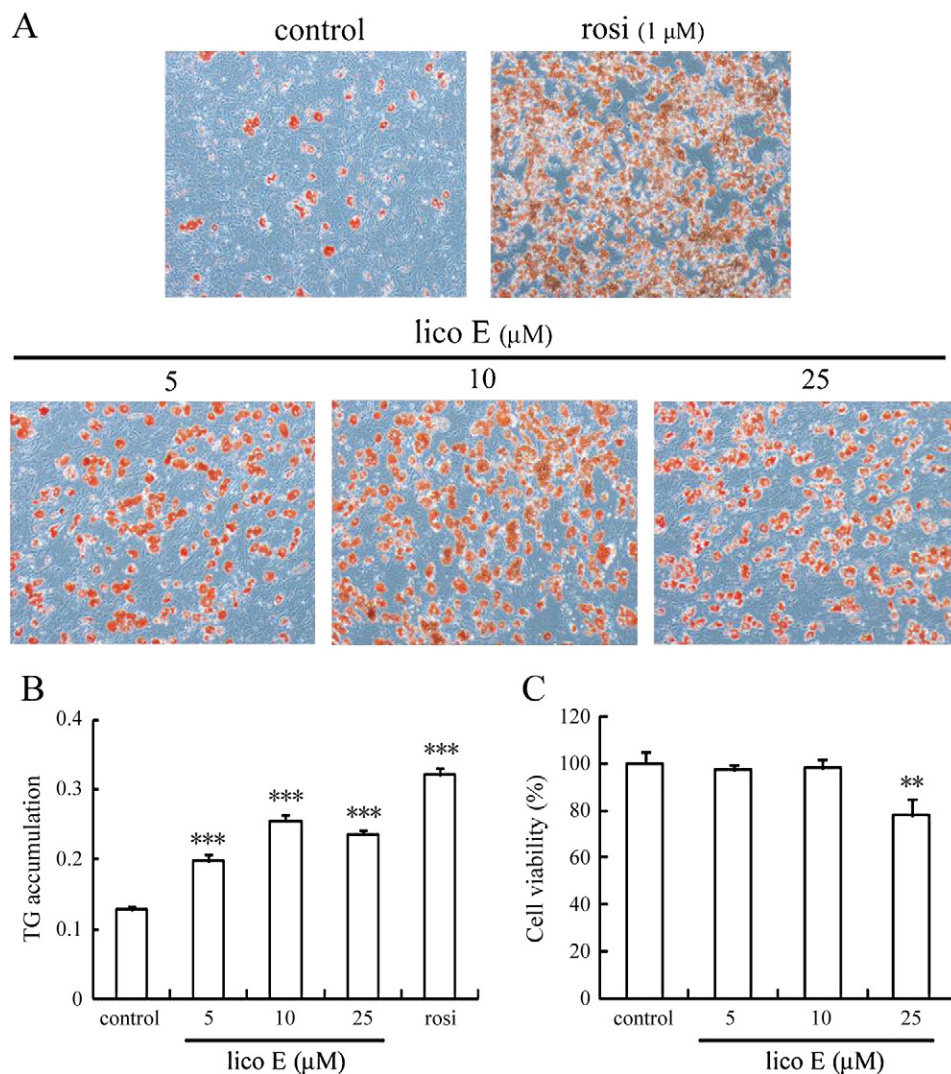


Fig. 2. Effects of lico E on adipocyte differentiation in C3H10T1/2. (A) C3H10T1/2 cells were treated with lico E (0, 5, 10 or 25 μM) during adipocyte differentiation for 8 days. Control was differentiated using standard adipogenic induction media without other treatment. The cells were stained with Oil Red O on day 8. Microscopic pictures were obtained at magnification of $\times 100$. (B) The stained Oil Red O was extracted with isopropanol. The absorbance of the extracted Oil Red O was spectrophotometrically determined at 570 nm to measure triglyceride accumulation. (C) To investigate the toxicity of lico E on cell viability, C3H10T1/2 was incubated in the presence of lico E at a concentration of 0, 5, 10 or 25 μM , and the cell viability was evaluated via MTT assays after 48 h. The error bars represent the standard error of the mean. The symbols ** and *** indicate significant difference at $P < .01$, and $P < .001$, respectively. TG, triglyceride.

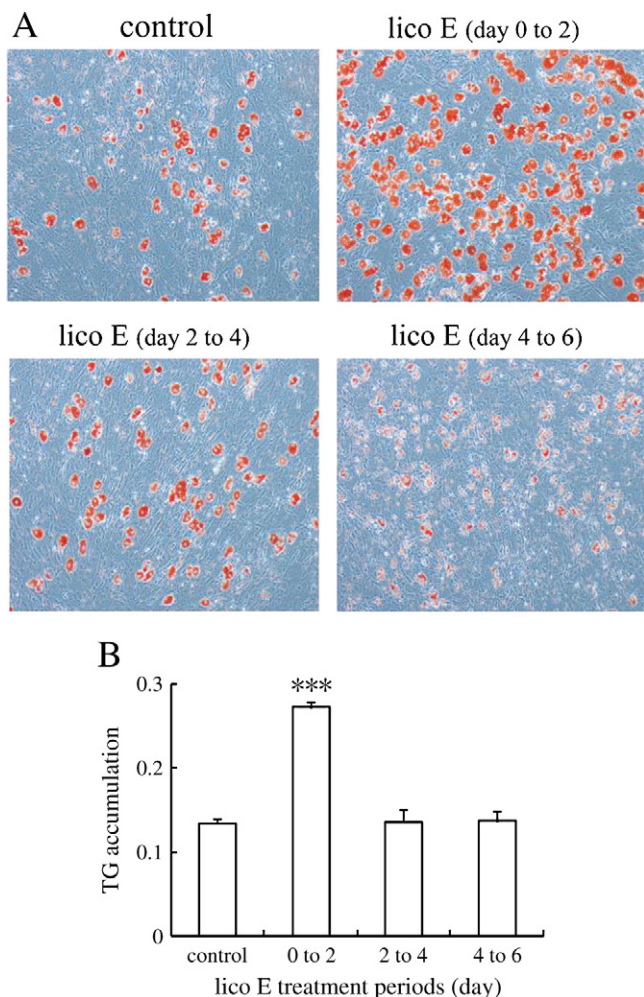


Fig. 3. The effects of lico E for various intervals during adipocyte differentiation. (A) C3H10T1/2 cells were treated with 10 mM lico E for various periods, and the controls were differentiated using standard adipogenic induction media without other treatments. The adipogenesis of C3H10T1/2 was visualized via Oil Red O staining. (B) The absorbance of the extracted Oil Red O was spectrophotometrically determined at 570 nm to measure triglyceride accumulation. The error bars represent the standard error of the mean. The symbol *** indicates a significant difference at $P < .001$. TG, triglyceride.

USA). Luciferase activities were normalized with β -galactosidase activity to adjust transfection efficiency.

2.5. Animal experiments

Five-week-old male C57BL/6J mice were purchased from Orient-Bio Inc. (Seoul, Korea). The animals were maintained in a temperature-controlled room at 22°C on a 12-h light–dark cycle. After 1 week of acclimation, mice were fed on a 58% high-fat diet (Research Diets, New Brunswick, NJ, USA) for 8 weeks. The glucose tolerance test (GTT) was conducted at 14 weeks of age to select diabetic mice, as described below. High-glucose mice were selected as the model diabetic mice and divided randomly into a control vehicle group ($n=5$) and a lico E group ($n=6$). For 2 weeks, the mice were intraperitoneally treated on a daily basis with vehicle (10% alcohol, 10% Tween 80 and 80% saline) alone or 10 mg/kg of lico E in the vehicle. After the administration of that treatment, GTT was again conducted, and blood samples were obtained for the subsequent biochemical analysis. For the experimental period, food intake and body weight were measured every day. Animal protocols were approved by the animal ethics committee of the Yonsei University College of Dentistry.

At necropsy, white adipose tissue (WAT) around epididymal or perirenal regions, and parenchymal organs such as the liver, heart and kidney were dissected and weighed. The WAT and liver were utilized for histological analysis, as described below.

2.6. Glucose tolerance test

Prior to and following treatment with vehicle or lico E, GTT was conducted as follows. The mice were fasted for 15 h and intraperitoneally injected with 2 g/kg

glucose. Blood glucose levels were measured with Accu-Check active systems (Roche, Mannheim, Germany) in accordance with the manufacturer's instructions at 0, 30, 60, 90 and 120 min after the glucose injection.

2.7. Serum biochemical analysis

Levels of triglycerides and cholesterol in serum were measured using a Hitachi H7170 automated analyzer (Hitachi Ltd., Tokyo, Japan). Concentrations of glutamic oxaloacetic transaminase (GOT) and glutamic pyruvic transaminase (GPT) were determined using GOT and GPT kits (Asan Pharmaceutical, Seoul, Korea), respectively, in accordance with the manufacturer's instructions.

2.8. Histological analysis

Dissected WAT and liver were fixed in 10% neutral-buffered formalin and embedded in paraffin. Paraffin-embedded sections were sliced at a width of 4 μ m and stained with hematoxylin and eosin. Adipocyte cell size was measured in seven randomly selected microscopic areas from five independent animals using an Olympus CKX41 inverted microscope system (Tokyo, Japan). The average adipocyte cell size was calculated by dividing the selected microscopic area by the total adipocyte cell number in the area.

2.9. Semiquantitative reverse transcription polymerase chain reaction (RT-PCR)

Total RNA in epididymal WAT (EWAT), perirenal WAT (PWAT) or C3H10T1/2 cells was isolated with Trizol reagent (Invitrogen, Carlsbad, CA, USA) in accordance with the manufacturer's instructions. Two micrograms of total RNA was converted to cDNA using an RT premix kit (Bioneer, Seoul, Korea) in accordance with the manufacturer's instructions. Semiquantitative RT-PCR was conducted in accordance with the protocols established in our previous studies [20,21]. In brief, two concentrations of cDNA template were amplified with i-StarTaq (Intron, Seoul, Korea) to determine the amounts of cDNA, and, additionally, several PCR cycles were conducted in an effort to determine the range during which amplification was in exponential phase. The primers, annealing temperatures and optimized PCR cycle number were determined in previous studies [20,21]. All assays were conducted in triplicate, and at least three separate assays were performed. The expression value of the control group was set as 1 to allow for the comparison of the relative mRNA expression levels between the control and lico E groups.

2.10. Western blot

For protein analysis, 250 mg of EWAT was homogenized in 1× lysis buffer [20 mM Tris-HCl (pH 7.5), 150 mM NaCl, 1 mM Na_2EDTA , 1% Triton, 2.5 mM sodium pyrophosphate, 1 mM β -glycerophosphate, 1 mM Na_3VO_4 , 1 μ g/ml leupeptin and 1 mM PMSF]. After centrifugation, the supernatant was used for the protein assay, and the remaining aliquot samples were stored at -70°C until use. Protein concentrations were determined with BSA protein assay kits (Bio-rad, Hercules, CA, USA). Thirty micrograms of protein was electrophoresed through 10% sodium dodecyl sulfate polyacrylamide gel electrophoresis. The electrophoretically separated protein electroblotted onto PVDF (Bio-rad). The membranes were blocked with 5% BSA in Tris buffer saline (10 mM Tris-HCl, 166 mM NaCl, pH 7.4). Primary antibodies were anti-phospho-Akt (Cell Signaling Technology, Beverly, MA, USA) at 1:1000, anti-phospho-Erk1/2 (Cell Signaling Technology) at 1:1000, anti-Akt (Cell Signaling Technology) at 1:1000 and anti-Erk1/2 (Cell Signaling Technology) at 1:1000. Secondary antibody was peroxidase-conjugated anti-rabbit (Jackson ImmunoResearch, West Grove, PA, USA) at 1:2500. Protein band was visualized by ECL kit (Amersham Bioscience, Buckinghamshire, UK). Band intensity was measured using Multi Gauge Ver 3.0 software (Fuji Film, Tokyo, Japan).

2.11. Statistical analysis

The SPSS 12.0 statistical package program (SPSS Inc., Chicago, IL, USA) was utilized for all statistical analyses. All data in the same groups were assessed via paired t tests. The data

Table 1
Changes of food intake, body weight and tissue weight in mice due to 2 weeks of lico E treatment

	Control group	Lico E group
Food intake (g/day)	2.45 \pm 0.09	2.43 \pm 0.09
Body weight before treatment	34.9 \pm 2.03	35.5 \pm 1.1
Body weight after treatment	37.8 \pm 1.95	37.8 \pm 2.75
Body weight increase (g)	2.9 \pm 1.03	2.3 \pm 1.17
EWAT (g)	2.11 \pm 0.12	2.27 \pm 0.1
PWAT (g)	1.01 \pm 0.11	0.94 \pm 0.02
Liver (g)	1.02 \pm 0.06	1.00 \pm 0.03
EWAT/body weight ratio	5.88 \pm 0.3	6.34 \pm 0.1
PWAT/body weight ratio	2.78 \pm 0.2	2.64 \pm 0.1
Liver/body weight ratio	2.83 \pm 0.1	2.80 \pm 0.06

Values are expressed as the means \pm standard error.

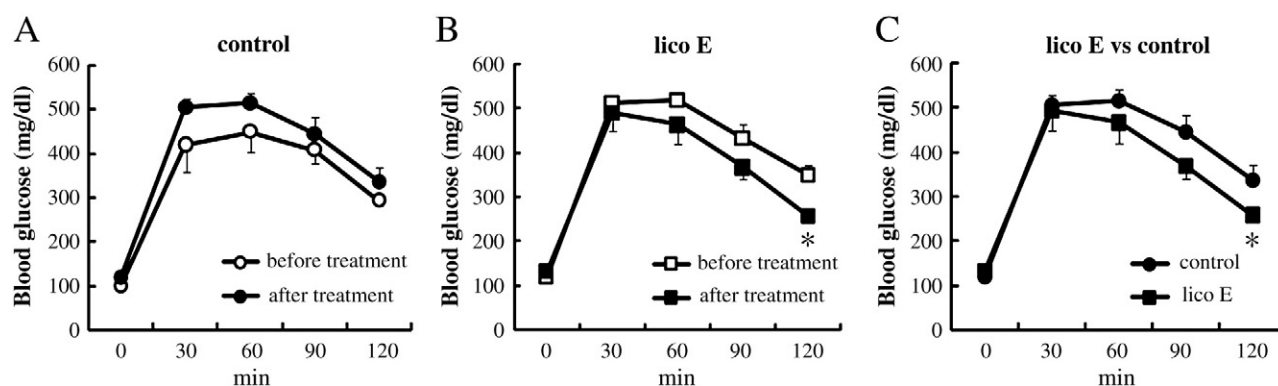


Fig. 4. Glucose tolerance test of diet-induced diabetic mice after lico E treatment. Licochalcone E dissolved in vehicle (10% alcohol, 10% Tween 80 and 80% saline) was intraperitoneally injected for 2 weeks. The control group was injected with vehicle alone. Blood glucose levels prior to treatment and after treatment in the control group (A) and the lico E group (B) are shown in the graph. (C) Blood glucose levels of the control group (●) vs. the lico E group (■) after treatment are shown in the graph. All values are expressed as means±standard errors. The symbol * indicates significant difference at $P<0.05$.

collected with the control and lico E groups were analyzed and compared via unpaired t tests. A P value of <0.05 was considered indicative of a statistically significant difference.

3. Results

3.1. Lico E induces the differentiation of 3T3-L1 preadipocyte

In order to evaluate the effects of lico E on the differentiation from preadipocytes to adipocytes, 3T3-L1 preadipocyte cells were incubated until 2 days postconfluence (day 0) and treated with lico E at a concentration of 0, 5, 10 or 20 μM for 8 days during a standard adipogenic induction. Rosi, a PPAR γ agonist, has been shown to promote adipocyte differentiation [23,24] and was therefore employed as a positive control in the *in vitro* study. As anticipated, rosi strongly induced adipocyte differentiation in 3T3-L1 as compared to the controls (Fig. 1A, B). The presence of lico E at 5 and 10 μM was shown to induce lipid accumulation both via microscopic examinations of Oil Red O-stained lipid droplets and by the spectrophotometric quantification of extracted stains (Fig. 1A, B), thereby indicating the induction of adipocyte differentiation. However, the induction disappeared at a lico E concentration of 20 μM . In order to evaluate the inhibitory effects of lico E on the cell viability of 3T3L1 preadipocytes, MTT assays were conducted after 48 h of treatment with lico E at a concentration of 0, 5, 10 or 20 μM (Fig. 1C). The results demonstrated that lico E exerted no effects on cell viability at concentrations of 5 and 10 μM ; however, the cell viability was slightly but significantly reduced at 20 μM (Fig. 1C), thereby suggesting that the inhibitory effect of 20 μM lico E on cell viability resulted in the disappearance of this induction of adipogenesis. Therefore, lico E at concentrations up to 10 μM induce differentiation from preadipocytes to adipocytes.

3.2. Lico E induces the differentiation of C3H10T1/2 multipotent stem cells

In order to characterize the effects of lico E on differentiation from multipotent stem cells to adipocytes, C3H10T1/2 stem cells were treated with lico E at a concentration of 0, 5, 10 or 25 μM for 8 days during a standard adipogenic induction. The presence of lico E at 5, 10 and 25 μM was shown to induce lipid accumulation both by microscopic examination and spectrophotometric quantification (Fig. 2A, B). The results of the MTT assay demonstrated that lico E did not alter cell viability up to a concentration of 10 μM , but cell viability was shown to be slightly but significantly reduced at 25 μM (Fig. 2C). Therefore, the optimal concentration of lico E in the C3H10T1/2 cells was defined as 10 μM , and so this concentration was utilized in the time-course study, as follows.

In an effort to elucidate the timing of the stimulatory effect of lico E on adipocyte differentiation, C3H10T1/2 cells were induced in the presence of 10 μM lico E for various periods. Licochalcone E treatment from day 0 to 2 after induction resulted in a significant induction of adipocyte differentiation (Fig. 3). By way of contrast, lico E treatment applied from day 2 to 4 and day 4s to 6 evidenced no apparent induction effects (Fig. 3). These results identified the period from day 0 to 2 as the critical time point for lico E treatment in order to induce adipogenesis. Therefore, the stimulatory effect of lico E on adipocyte differentiation occurs at the early stages of adipocyte differentiation.

3.3. No gross changes on food intake and body weight

In order to examine gross changes of diet-induced diabetic mice during 10-mg/kg/day lico E treatment, we measured the food intake and body weight every day during the experimental period (Table 1). The body weight gain in the lico E group (2.3 ± 1.17 g) was similar to that in the control group (2.9 ± 1.03 g), and the food intake of the lico E group (2.43 ± 0.09 g/day) was also found to be similar to that of the control group (2.45 ± 0.09 g/day). Therefore, 2 weeks of lico E treatment did not affect food intake or body weight, and thus no gross body changes were observed in this study.

3.4. Lico E improves glucose tolerance and lipid metabolism

In order to determine whether lico E exerts an antidiabetic effect, serum biochemical analyses of blood glucose, triglyceride and cholesterol were conducted after 15 h of fasting (Fig. 4 and Table 2). The control mice treated for 2 weeks with vehicle evidenced a trend, albeit a statistically significant one, toward higher blood glucose levels after 30 min, thereby suggesting that the diabetic condition of the control mice may worsen (Fig. 4A). Of particular importance, the blood glucose tolerance level in the lico E group was improved significantly after 2 weeks of treatment (Fig. 4B, C). The blood glucose levels began

Table 2
Serum biochemical parameters in mice with 2 weeks of lico E treatment

	Control group	Lico E group
Triglyceride (mg/dl)	93.36 ± 17.33	$59.33\pm2.73^*$
Cholesterol (mg/dl)	118.38 ± 9.40	124.02 ± 5.23
GPT (IU/L)	6.06 ± 0.6	6.85 ± 2.5
GOT (IU/L)	31.39 ± 3.58	32.00 ± 3.8

Values are expressed as the means±standard error.

* $P<0.05$; significantly different from control group.

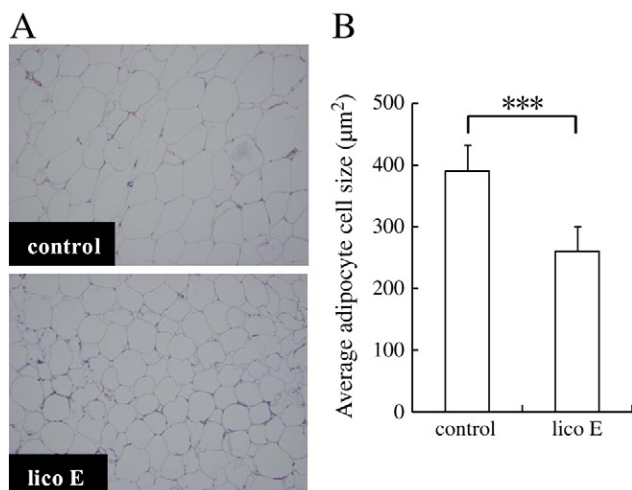


Fig. 5. Histological analysis of WATs of DIO mice after control or lico E treatments for 14 days. (A) Histological sections were stained with hematoxylin and eosin. Microscopic pictures of EWAT of control or lico E groups were obtained at magnification of $\times 200$. (B) An average adipocyte cell size in EWAT of control and lico E groups was quantified by measurements conducted in randomly selected microscopic areas. The error bars represent the standard error of the mean. The symbol *** indicates a significant difference at $P < .001$.

to decrease at 60 min and were significantly lower at 120 min ($P < .05$), thereby indicating that lico E exerts a blood-glucose-lowering effect.

The results of serum biochemical analysis are provided in Table 2. The level of serum triglycerides in the lico E group (59.33 ± 2.73 , $P < .05$) was reduced significantly as compared to that in the control group (93.36 ± 17.33), thereby suggesting that lico E treatment ameliorates hyperlipidemia in diabetic mice. The levels of total cholesterol were similar between the two groups (control: 118.38 ± 9.40 and lico E: 124.02 ± 5.23). Taken together, our results demonstrate that lico E treatment improves glucose tolerance and lipid metabolism, thereby suggesting that lico E exerts an antidiabetic effect.

Additionally, the liver damage indices, GOT and GPT, were analyzed (Table 2). The levels of GOT and GPT in the lico E group were 32 ± 3.8 and 6.85 ± 2.5 , respectively, whereas the levels in the control group were 31.39 ± 3.58 and 6.06 ± 0.6 . The levels of GOT and GPT in both groups were similarly maintained at normal levels, thereby suggesting that lico E treatment did not evidence toxicity in the liver.

3.5. No weight changes in WAT and internal organs

To evaluate the internal organ changes of diet-induced diabetic mice as the result of lico E treatment, the animals were weighed and sacrificed at the end of the treatment period. Epididymal WAT, PWAT, liver, kidney and heart were dissected and weighed, and the tissue weight/body weight ratios were calculated. The weights and the ratios to body weight of EWAT and PWAT were similar between the control and lico E groups (Table 1). Additionally, the weight and ratio to body weight of parenchymal tissues such as the liver, heart and kidney did not evidence a significant difference between the two groups (Table 1 for liver, and data of heart and kidney not shown).

3.6. Lico E decreases adipocyte size of WAT

The reduction of adipocyte size in the EWAT and PWAT of the lico E group was noted on histopathological analysis (Fig. 5A for EWAT; PWAT not shown). Adipocyte size in EWAT was quantified by measurements conducted in randomly selected microscopic areas and was markedly decreased by 33.4%, in the lico E group as compared with the control group ($P < .001$) (Fig. 5B). This suggested that lico E treatment may improve histological morphology in WAT. Additionally, histological analysis of the liver showed no differences in histopathological appearance between the two groups, consistent with the unchanged levels of GOT and GPT (data not shown).

3.7. Lico E increases PPAR γ expression in WAT

Because lico E increased adipocyte differentiation *in vitro* and reduced adipocyte size *in vivo*, we assessed the effects of lico E on the expression of adipocyte marker genes in WAT. The mRNA expression levels of adipocyte marker genes, PPAR γ , aP2 and C/EBP α , were measured via semiquantitative RT-PCR (Fig. 6). Licochalcone E markedly increased PPAR γ mRNA expression to 1.78-fold in EWAT and 1.72-fold in PWAT ($P < .05$ in EWAT and $P < .01$ in PWAT) (Fig. 6), whereas the gene expression of aP2 and C/EBP α was measured at similar levels in both the lico E and control groups. The significant up-regulation of PPAR γ expression as the result of lico E treatment may induce adipocyte differentiation and thus decrease adipocyte size *in vivo*.

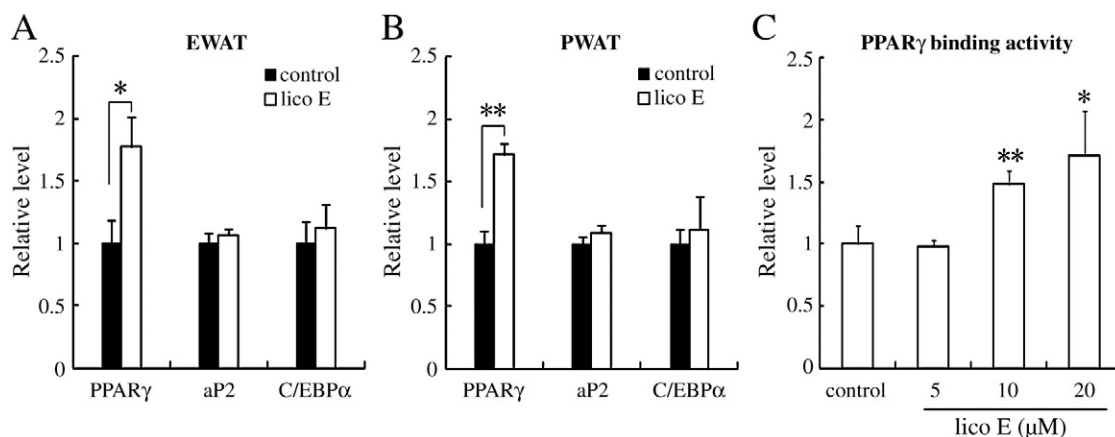


Fig. 6. The expressions of adipogenic marker genes in WATs and PPAR γ ligand-binding activity of lico E. Messenger RNA expression levels of adipogenic marker genes in EWAT (A) and PWAT (B) were evaluated via RT-PCR. The relative mRNA expression levels of control (■) vs. lico E (□) are shown in the graph. The expression value of the control group was set as 1 to permit comparison of the relative mRNA expression levels between the control and lico E groups. (C) CV1 cells (monkey kidney cell line) were transfected with pUSA-luciferase, GAL4PPAR γ LBD and CMV β -galactosidase. Transfected cells were treated after 24 h with lico E at a concentration of 0, 5, 10 and 20 μM. Luciferase activity was measured after 24 h using the luciferase substrate. The error bars represent the standard error of the mean. The symbols * and ** indicate significant difference at $P < .05$ and $P < .01$, respectively. C/EBP α , CAAT enhancer binding protein α ; aP2, fatty-acid-binding protein.

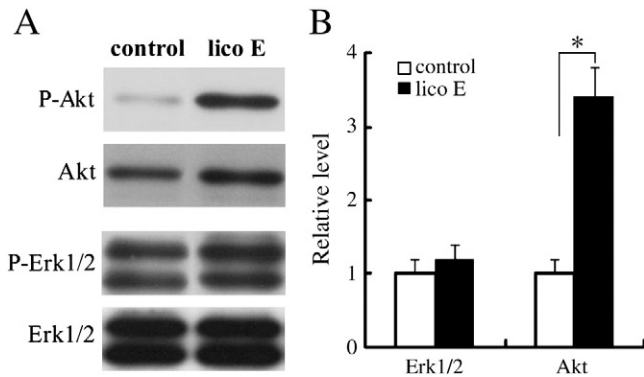


Fig. 7. Activation of Erk1/2 and Akt in EWAT was detected via Western blotting. (A) The phosphorylation of Erk1/2 and Akt was compared with the total levels of Erk1/2 and Akt in the loading controls, respectively. Band intensities were plotted as a relative fold increase. (B) The relatively protein levels of control (□) vs. lico E (■) are shown in the graph. The error bars represent the standard error of the mean. The symbol * indicates significant difference at $P < 0.05$.

3.8. PPAR γ ligand-binding activity of lico E

As PPAR γ mRNA expression was shown in this study to be enhanced by lico E and ethanolic licorice extract was reported to function as a PPAR γ agonist [25], the effects of lico E on the transactivation of PPAR γ were evaluated. The level of PPAR γ transactivation indicates the degree to which lico E binds to and activates PPAR γ as its agonist. CV1 cells were co-transfected with pUSA-luciferase, GAL4PPAR γ LBD and CMV β -galactosidase [26–28]. The transfected CV1 cells were treated with lico E at a concentration of 0, 5, 10 or 20 μ M, and the PPAR γ transactivation activity was determined by the luciferase activity. Licorice extract enhanced PPAR γ transactivation in a dose-dependent manner (Fig. 6C). The results demonstrated that PPAR γ transactivation as the result of lico E at a concentration of 20 μ M was significantly increased to a level 1.7-fold

that of the controls (Fig. 6C). Compared to the 16.5-fold increase of the full agonist rosi (data not shown), lico E was shown to be a much weaker transactivator of PPAR γ , as indicated by its lower transactivation activity (10.3% of that observed with rosi), thereby indicating that lico E is a weak partial PPAR γ agonist.

3.9. Lico E enhances the Akt phosphorylation associated with insulin signaling in WAT

To obtain further insight into the molecular mechanism underlying the improved glucose tolerance in the lico E group, we determined the levels of total protein and phosphorylated protein of Erk1/2 and Akt in EWAT, which perform important roles in glucose metabolism, such as insulin signaling and adipogenesis (Fig. 7). The level of Akt phosphorylation in the lico E group was increased significantly – by about 3.4-fold – as compared with that measured in the control group, whereas the level of Erk phosphorylation in the lico E group was not found to differ significantly (1.2-fold). These data indicated that lico E treatment up-regulates Akt signaling to a significant degree in the EWAT.

3.10. Induction of adipocyte differentiation by lico E requires Akt signal pathway

In order to evaluate how important Akt signal pathway is for the induction of adipocyte differentiation and PPAR γ expression by lico E, C3H10T1/2 cells were pretreated with 10 μ M Akt inhibitor for 1 h before the cells were stimulated to differentiate in the standard adipocyte medium containing 10 μ M lico E and 10 μ M Akt inhibitor. Akt inhibitor significantly inhibited the lipid accumulation induced by lico E (Fig. 8A). In addition, the mRNA expression level of PPAR γ increased by lico E was significantly reduced in the presence of Akt inhibitor (Fig. 8B). These results suggest that Akt signal pathway is involved in the adipocyte differentiation and mRNA expression level of PPAR γ is induced by lico E.

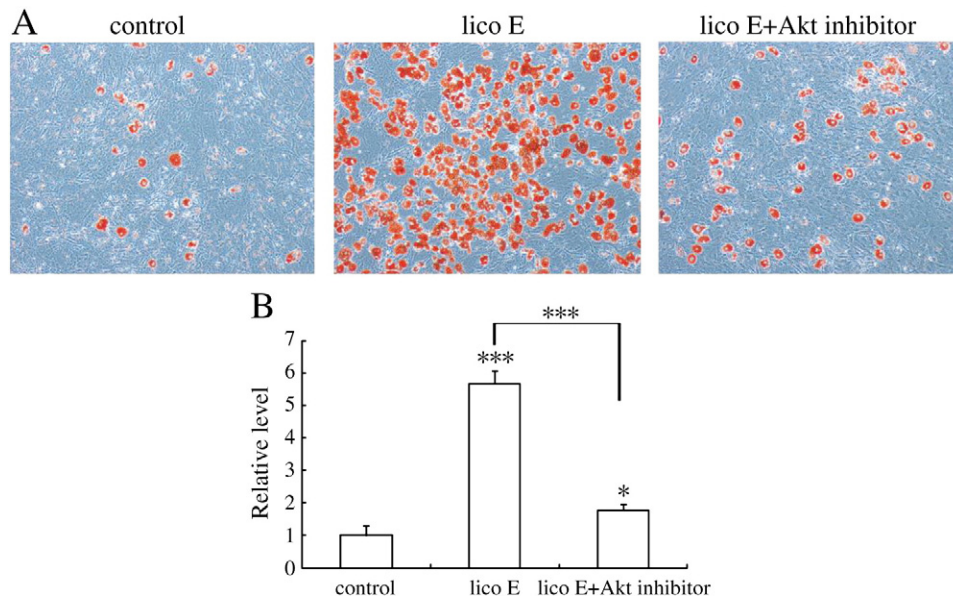


Fig. 8. Effects of Akt inhibitor on the induction of adipocyte differentiation and PPAR γ expression level by lico E in C3H10T1/2. (A) C3H10T1/2 cells were treated with 10 μ M lico E during adipocyte differentiation for 8 days. In case of Akt inhibitor treatment, C3H10T1/2 cells were pretreated with 10 μ M Akt inhibitor for 1 h before differentiation with lico E and Akt inhibitor. Control was differentiated using standard adipogenic induction media without other treatment. The cells were stained with Oil Red O on day 8. Microscopic pictures were obtained at magnification of $\times 100$. (B) Messenger RNA expression levels of PPAR γ gene in lico E and lico E + Akt inhibitor were evaluated via RT-PCR. The relatively mRNA expression levels of control vs. lico E, and control vs. lico E + Akt inhibitor are shown in the graph. The expression value of the control group was set as 1 to permit comparison of the relative mRNA expression levels. The symbols * and *** indicate significant difference at $P < 0.05$ and $P < 0.001$, respectively.

4. Discussion

Previously, high-dose administration (100–300 mg/kg/day) of the licorice ethanolic extract was found to ameliorate diabetes in a diabetic animal model; additionally, the licorice extract evidenced PPAR γ ligand-binding activity *in vitro* [25]. Recently, lico E was shown to inhibit protein tyrosine phosphatase 1B (PTP1B), which performs a critical function in the negative regulation of the insulin and leptin signaling pathways [29], and the inhibition of PTP1B activity appears to be a promising novel therapeutic target for type 2 diabetes. Considering the accumulating evidence suggesting that lico E may exert an antidiabetic effect, we evaluated the biological effects of lico E on adipocyte differentiation *in vitro* and antidiabetic activity in a diabetic animal model.

The results of this study showed that lico E induces lipid accumulation during adipogenesis in 3T3-L1 preadipocytes and C3H10T1/2 stem cells, thereby indicating that lico E induces adipocyte differentiation. Additionally, the time-course study revealed a strict temporal requirement for the effects of lico E on adipocyte differentiation. Licochalcone E exerts an induction effect on adipocyte differentiation at the early induction stage, but no effect at later stages. These results show that lico E regulates the adipogenic process during early stages and performs a crucial function in adipocyte differentiation.

Diet-induced diabetic mice were used to demonstrate the antidiabetic effects of lico E on type 2 diabetes. Licochalcone E did not affect body weight or food intake over a period of 2 weeks, revealing that the effects noted in the *in vivo* study were not attributable to changes in weight or appetite. Licochalcone E evidenced a blood-glucose-lowering effect and a serum triglyceride-decreasing effect that should be beneficial in improving hyperglycemia and hyperlipidemia under diabetic conditions. Therefore, lico E exerts an antidiabetic effect.

The reduction of adipocyte size by lico E treatment was observed via histological analysis in the WAT, whereas the WAT weight and the ratios to body weight remained unchanged. This result suggests that lico E increases the population of small adipocytes in WAT. Additionally, our data indicated that lico E functions as a weak partial PPAR γ agonist and that lico E treatment induces the expression of PPAR γ mRNA in WAT.

Akt signaling activation is involved in stimulations of glycogen synthesis, protein synthesis, cell survival, the inhibition of lipolysis and glucose uptake. Therefore, the activation of Akt is considered crucial for adipogenesis [30,31]. Akt activation is markedly impaired in diabetic humans and rodents, and the normalization of hyperglycemia is correlated with the restoration of Akt activity [32,33]. In this study, we determined that lico E treatment stimulates Akt signaling in EWAT, and Akt signal pathway is necessary for the induction of both adipocyte differentiation and PPAR γ gene expression by lico E in C3H10T1/2 adipocyte differentiation. Akt stimulation by lico E may contribute to improved Akt signaling and hyperglycemia previously impaired by diabetic conditions. Consistent with our findings, the Akt signal cascade was shown to induce PPAR γ expression during the induction of 3T3-L1 adipocyte differentiation [34,35], and the stimulation of Akt activity was parallel to PPAR γ expression and enhanced preadipocyte differentiation [36,37]. Based on these results, it can be speculated that lico E increases PPAR γ expression level via the stimulation of Akt signaling and also functions as a partial agonist of PPAR γ , and the increased PPAR γ expression enhances the adipocyte differentiation and population of small adipocytes, thereby resulting in the improvement of hyperglycemia and hyperlipidemia under diabetic conditions.

In conclusion, the results of this study demonstrated that lico E enhances adipocyte differentiation at the early induction stage during adipogenesis and evidences antidiabetic activity in diabetic mice. Our findings that PPAR γ expression and Akt activation are enhanced by

lico E treatment contribute to our understanding of the mechanisms underlying the antidiabetic effects of lico E. To the best of our knowledge, this is the first report to demonstrate the effects of lico E on the metabolic properties associated with diabetes.

Acknowledgments

This work was supported by the Priority Research Centers Program through the National Research Foundation of Korea (NRF) funded by the Ministry of Education, Science and Technology (2010-0029702).

References

- [1] Frayn KN. Adipose tissue and the insulin resistance syndrome. *Proc Nutr Soc* 2001;60:375–80.
- [2] Yu ZK, Wright JT, Hausman GJ. Preadipocyte recruitment in stromal vascular cultures after depletion of committed preadipocytes by immunocytotoxicity. *Obes Res* 1997;5:9–15.
- [3] Young HE, Mancini ML, Wright RP, Smith JC, Black Jr AC, Reagan CR, et al. Mesenchymal stem cells reside within the connective tissues of many organs. *Dev Dyn* 1995;202:137–44.
- [4] Caplan AL. Mesenchymal stem cells. *J Orthop Res* 1991;9:641–50.
- [5] Green H, Kehinde O. Sublines of mouse 3T3 cells that accumulate lipid. *Cell* 1974;1:113–5.
- [6] Green H, Kehinde O. An established preadipose cell line and its differentiation in culture. II. Factors affecting the adipose conversion. *Cell* 1975;5:19–27.
- [7] Green H, Kehinde O. Spontaneous heritable changes leading to increased adipose conversion in 3T3 cells. *Cell* 1976;7:105–13.
- [8] Reznikoff CA, Brankow DW, Heidelberger C. Establishment and characterization of a cloned line of C3H mouse embryo cells sensitive to postconfluence inhibition of division. *Cancer Res* 1973;33:3231–8.
- [9] Pinney DF, Emerson Jr CP. 10T1/2 cells: an *in vitro* model for molecular genetic analysis of mesodermal determination and differentiation. *Environ Health Perspect* 1989;80:221–7.
- [10] Bowers RR, Kim JW, Otto TC, Lane MD. Stable stem cell commitment to the adipocyte lineage by inhibition of DNA methylation: role of the BMP-4 gene. *Proc Natl Acad Sci U S A* 2006;103:13022–7.
- [11] Olefsky JM. The effects of spontaneous obesity on insulin binding, glucose transport, and glucose oxidation of isolated rat adipocytes. *J Clin Invest* 1976;57:842–51.
- [12] Sreenan S, Sturis J, Pugh W, Burant CF, Polonsky KS. Prevention of hyperglycemia in the Zucker diabetic fatty rat by treatment with metformin or troglitazone. *Am J Physiol* 1996;271:E742–7.
- [13] Stevenson RW, Hutson NJ, Krupp MN, Volkmann RA, Holland GF, Eggler JF, et al. Actions of novel antidiabetic agent englitazone in hyperglycemic hyperinsulinemic ob/ob mice. *Diabetes* 1990;39:1218–27.
- [14] Koren S, Fantus IG. Inhibition of the protein tyrosine phosphatase PTP1B: potential therapy for obesity, insulin resistance and type-2 diabetes mellitus. *Best Pract Res Clin Endocrinol Metab* 2007;21:621–40.
- [15] Montalibet J, Kennedy BP. Therapeutic strategies for targeting PTP1B in diabetes. *Drug Discovery Today: Therapeutic Strategies* 2005;2:129–35.
- [16] Ayabe SI, Yoshikawa T, Kobayashi M, Furuya T. Biosynthesis of a retrochalcone, echinatin: involvement of O-methyltransferase to licodione. *Phytochemistry* 1980;19:2331–6.
- [17] Yoon G, Jung YD, Cheon SH. Cytotoxic allyl retrochalcone from the roots of *Glycyrrhiza inflata*. *Chem Pharm Bull (Tokyo)* 2005;53:694–5.
- [18] Na Y, Cha JH, Yoon HG, Kwon Y. A concise synthesis of licochalcone E and its regio-isomer, licochalcone F. *Chem Pharm Bull (Tokyo)* 2009;57:607–9.
- [19] Student AK, Hsu RY, Lane MD. Induction of fatty acid synthetase synthesis in differentiating 3T3-L1 preadipocytes. *J Biol Chem* 1980;255:4745–50.
- [20] Lee JS, Suh JM, Park HG, Bak EJ, Yoo YJ, Cha JH. Heparin-binding epidermal growth factor-like growth factor inhibits adipocyte differentiation at commitment and early induction stages. *Differentiation* 2008;76:478–87.
- [21] Bak EJ, Park HG, Kim JM, Kim JM, Yoo YJ, Cha JH. Inhibitory effect of evodiamine alone and in combination with rosiglitazone on *in vitro* adipocyte differentiation and *in vivo* obesity related to diabetes. *Int J Obes (Lond)* 2010;34:250–60.
- [22] Kim JB, Wright HM, Wright M, Spiegelman BM. ADD1/SREBP1 activates PPAR γ through the production of endogenous ligand. *Proc Natl Acad Sci U S A* 1998;95:4333–7.
- [23] Madsen L, Petersen RK, Sorensen MB, Jorgensen C, Hallenborg P, Pridal L, et al. Adipocyte differentiation of 3T3-L1 preadipocytes is dependent on lipoxygenase activity during the initial stages of the differentiation process. *Biochem J* 2003;375:539–49.
- [24] Nugent C, Prins JB, Whitehead JP, Savage D, Wentworth JM, Chatterjee VK, et al. Potentiation of glucose uptake in 3T3-L1 adipocytes by PPAR gamma agonists is maintained in cells expressing a PPAR gamma dominant-negative mutant: evidence for selectivity in the downstream responses to PPAR gamma activation. *Mol Endocrinol* 2001;15:1729–38.
- [25] Mae T, Kishida H, Nishiyama T, Tsukagawa M, Konishi E, Kuroda M, et al. A licorice ethanolic extract with peroxisome proliferator-activated receptor-gamma ligand-

- binding activity affects diabetes in KK-Ay mice, abdominal obesity in diet-induced obese C57BL mice and hypertension in spontaneously hypertensive rats. *J Nutr* 2003;133:3369–77.
- [26] Kim TH, Kim H, Park JM, Im SS, Bae JS, Kim MY, et al. Interrelationship between liver X receptor alpha, sterol regulatory element-binding protein-1c, peroxisome proliferator-activated receptor gamma, and small heterodimer partner in the transcriptional regulation of glucokinase gene expression in liver. *J Biol Chem* 2009;284:15071–83.
- [27] Takahashi N, Kawada T, Goto T, Yamamoto T, Taimatsu A, Matsui N, et al. Dual action of isoprenols from herbal medicines on both PPARgamma and PPARalpha in 3T3-L1 adipocytes and HepG2 hepatocytes. *FEBS Lett* 2002;514:315–22.
- [28] Kliewer SA, Forman BM, Blumberg B, Ong ES, Borgmeyer U, Mangelsdorf DJ, et al. Differential expression and activation of a family of murine peroxisome proliferator-activated receptors. *Proc Natl Acad Sci U S A* 1994;91:7355–9.
- [29] Yoon G, Lee W, Kim SN, Cheon SH. Inhibitory effect of chalcones and their derivatives from *Glycyrrhiza inflata* on protein tyrosine phosphatase 1B. *Bioorg Med Chem Lett* 2009;19:5155–7.
- [30] Sakaue H, Ogawa W, Matsumoto M, Kuroda S, Takata M, Sugimoto T, et al. Posttranscriptional control of adipocyte differentiation through activation of phosphoinositide 3-kinase. *J Biol Chem* 1998;273:28945–52.
- [31] Whiteman EL, Cho H, Birnbaum MJ. Role of Akt/protein kinase B in metabolism. *Trends Endocrinol Metab* 2002;13:444–51.
- [32] Krook A, Kawano Y, Song XM, Efendic S, Roth RA, Wallberg-Henriksson H, et al. Improved glucose tolerance restores insulin-stimulated Akt kinase activity and glucose transport in skeletal muscle from diabetic Goto-Kakizaki rats. *Diabetes* 1997;46:2110–4.
- [33] Krook A, Roth RA, Jiang XJ, Zierath JR, Wallberg-Henriksson H. Insulin-stimulated Akt kinase activity is reduced in skeletal muscle from NIDDM subjects. *Diabetes* 1998;47:1281–6.
- [34] Park SY, Shin HK, Lee JH, Kim CD, Lee WS, Rhim BY, et al. Cilostazol ameliorates metabolic abnormalities with suppression of proinflammatory markers in a db/db mouse model of type 2 diabetes via activation of peroxisome proliferator-activated receptor gamma transcription. *J Pharmacol Exp Ther* 2009;329:571–9.
- [35] Fritzius T, Moelling K. Akt- and Foxo1-interacting WD-repeat-FYVE protein promotes adipogenesis. *EMBO J* 2008;27:1399–410.
- [36] Peng XD, Xu PZ, Chen ML, Hahn-Windgassen A, Skeen J, Jacobs J, et al. Dwarfism, impaired skin development, skeletal muscle atrophy, delayed bone development, and impeded adipogenesis in mice lacking Akt1 and Akt2. *Genes Dev* 2003;17:1352–65.
- [37] Baudry A, Yang ZZ, Hemmings BA. PKBalpha is required for adipose differentiation of mouse embryonic fibroblasts. *J Cell Sci* 2006;119:889–97.